J. Phys.: Condens. Matter **11** (1999) 5845–5853. Printed in the UK PII: S0953-8984(99)02252-3

Evidence of relaxation of Jahn–Teller polarons above T_C in $La_{1-x}Sr_xMnO_3$ ($0.1 < x \leqslant 0.5$)

Dipten Bhattacharya§†, Amitava Chakraborty‡ and H S Maiti‡

† Cryogenic Division, National Physical Laboratory, Dr K S Krishnan Road, New Delhi 110 012, India

‡ Electroceramics Laboratory, Central Glass and Ceramic Research Institute, Calcutta 700 032, India

E-mail: dipten@csnpl.ren.nic.in

Received 2 March 1999, in final form 19 May 1999

Abstract. We report the resistivity (ρ)–temperature (T) patterns in $La_{1-x}Sr_xMnO_3$ ($0.1 < x \leqslant 0.5$) systems over a temperature regime of 20–1273 K. Apart from a general trend of metallic ρ–T pattern below T_C (Curie point) and insulating above it, we have observed a re-entrant metallic ρ–T pattern beyond a characteristic temperature T^* above T_C for the compositions $0.25 \leqslant x \leqslant 0.50$. Such behaviour possibly reflects the relaxation of Jahn–Teller (JT) polarons (which form as a result of splitting of Mn^{3+} 3d outer levels and associated distortion in MnO_6 octahedra) at a higher temperature. The polaron formation energy E_{JT} has been calculated from fitting a simple two-channel conduction model with the resistivity data. It appears to vary significantly with the Sr^{2+} ion concentration (x) or the concentration of JT-active Mn^{3+} ions which reflects the variation of the extent of Jahn–Teller coupling. The relaxation of polarons and the change in the behaviour of ρ–T pattern above T^* are not associated with any commensurate magnetic transition which seems to be supporting the notion that Jahn–Teller polarons influence the properties like T_C, conductivity, magnetoresistivity etc significantly.

1. Introduction

The magnetoresistive behaviours of the perovskite $La_{1-x}A_xMnO_3$ (A = Sr/Ba/Ca etc) family of materials have recently been explored in detail [1-3]. Colossal magnetoresistance from 40% to 100 000% has been observed in these materials either in the bulk form or in the thin film form. These observations have brighten the prospect of utilizing the materials as different magnetic sensors. Substitution of La^{3+} in parent $LaMnO_3$ by divalent Sr, Ba or Ca creates holes at Mn^{3+} and drives an antiferromagnetic to ferromagnetic and insulating to metal transition around a doping level $x \approx 0.2$. Traditionally, the strong correlation between the ferromagnetic and metallic behaviours is explained by a concept of double exchange interaction [4]. According to this concept, the hopping of the holes at Mn^{4+} to Mn^{3+} via O^{2-} is associated with the lining up of localized spins at Mn sites in parallelism. Although, this mechanism explains much of the experimental observations on electrical transport and magnetic behaviours, there are quite a few anomalies as well. Quantitative estimation of T_C (Curie point) following the double exchange model reveals almost an order of magnitude higher values than what is observed experimentally. There are discrepancies in the magnitude of resistivity and magnetoresistivity (near T_C) as well, between the calculated values and the observed ones. These discrepancies have been attributed

§ Author to whom correspondence should be addressed.

0953-8984/99/305845+09$30.00

to the Jahn–Teller splitting of outer Mn d levels in Mn^{3+} ions and consequent reduction in electron kinetic energy [5]. Evidences have recently been piled up in favour of formation of Jahn–Teller (JT) polarons (charge carriers coupled with local lattice distortions) and many consequences of JT polarons are shown: a giant isotope effect on T_C [6], signatures in EPR spectra [7], optical studies [8], transport properties [9] etc.

In recent works, it has also been pointed out that the $La_{1-x}Sr_xMnO_3$ family of materials are charge transfer insulators where the hole is doped at O^{2-} [10], strong electron–phonon or electron–electron correlation effects are present even below T_C [11] and, therefore, the double exchange mechanism is not sufficient to describe the properties in that temperature regime also. It appears that the charge transport and magnetization properties are governed by the charge, orbital and spin ordering and their complex interplay over the entire phase diagram [12]. There are, at least, three concepts which have been proposed so far in order to explain the conductivity and magnetization over a wider temperature range: (i) formation of simple JT polarons [5], (ii) formation of spin polarons with two manganese ions around a JT ion [13] and (ii) formation of lattice bipolarons and their collapse below T_C [14].

In this paper, we report the resistivity–temperature patterns of the $La_{1-x}Sr_xMnO_3$ ($0.1 < x \leqslant 0.5$) family over a wide temperature range 20–1273 K. We have observed a re-entrant metallic ρ–T pattern above a characteristic temperature T^* (which is higher than T_C) within the composition range $0.25 \leqslant x \leqslant 0.5$. This seems to be evidence of the formation of JT polarons and their relaxation at higher temperatures (above T_C) as T^* drops sharply with the increase in x or, in other words, with the decrease in JT-active Mn^{3+} ions. The binding energy of the JT polarons E_{JT} is calculated as a function of doping level x from fitting a two-channel conduction model (which takes care of ferromagnetism-driven metallicity below T_C and activated hopping conduction above T_C) with the experimental data over the entire temperature range. E_{JT}, too, appears to drop significantly with x and is found to be varying over 0.019 eV to 0.0806 eV. Therefore, the most plausible explanation for the re-entrant metallic ρ–T pattern beyond T^* seems to be the change in the size and mobility of the small polarons around the JT-active ions.

2. Experiment

Sintered $La_{1-x}Sr_xMnO_3$ samples have been prepared by a process of compaction of the powder and subsequent sintering. The powder is prepared by autoignition of a gel at a relatively low temperature ($\sim$180 °C). The gel is formed after sufficient boiling of a mixture of aqueous metal nitrate solution (metal ions are taken in proper stoichiometric proportion) and a citric acid solution. The details of the powder preparation procedure, characterizations of the powder (particle size distribution, compositional homogeneity, phase purity etc), and the characterization of the sintered product (phase purity, compositional mapping, oxygen vacancies etc) have been reported elsewhere [15–17]. Phase purity of the sintered samples has been thoroughly verified by detailed x-ray diffraction studies. The Mn^{4+} concentration in the samples has been verified by the chemical analysis [18]. The variation from the nominal composition for these samples (in the composition range $\sim$0.16–0.50) is very small ($\sim$1–2%). The resistivity (ρ)–temperature (T) behaviours of the samples over a temperature range 20–1273 K have been observed. Resistivity patterns between 20 and 300 K were measured in a set-up connected with a cryocooler of CTI, Cryogenics, Inc. Silver contact points were used in the standard four-probe configuration for the resistivity measurements. The measurements over a temperature range 300–1273 K have been carried out in a resistance furnace. Platinum contact points were used for all the high temperature measurements. The oxygen content is important in these materials since the change in oxygen concentration (which may take place at

higher temperature) leads to a change in the charge carrier concentration. The measurements, however, have been carried out under normal atmospheric conditions and no oxygen loss is observed during heating up to the maximum temperature limit ($\sim$1000 °C) within which the measurements have been carried out. This is verified through thermogravimetric analysis also, up to 1000 °C. The resistivity plots are found to be reversible. This has been observed in this class of materials by others as well [19, 20]. Magnetic measurements up to a temperature 300 K were carried out in a vibrating sample magnetometer (VSM) of DMS, Inc.

3. Results and discussion

The resistivity (ρ)–temperature (T) plots for the $La_{1-x}Sr_xMnO_3$ samples with different x ($\approx$0.16–0.5) or Sr concentration are shown in figure 1. The general pattern for all the samples is the metallic ρ–T below T_C and the insulating ρ–T above T_C. This is a commonly observed behaviour widely reported in the literature [1–3]. However, there are quite a few interesting features in the ρ–T patterns over the entire temperature regime: (i) in the sample with $x = 0.16$, an upturn in ρ–T at a low temperature (< 120 K) is observed which is possibly a reflection of type-A antiferromagnetism-driven insulating behaviour [21]; (ii) in the samples with $x = 0.25$–0.5, beyond a characteristic temperature T^* (which is higher than T_C), a re-entrant metallic ρ–T pattern is observed; (iii) the difference between T_C and T^* decreases with the increase in x.

The conductivity of these compounds over such a wide temperature range is governed by the interplay of charge, orbital and spin degrees of freedom. Even below T_C, a strong incoherent scattering background is observed in the optical conductivity $\sigma(\omega)$ which highlights the inadequacies of the simple double exchange mechanism [11]. In spite of such an anomaly, it has been observed that ρ scales with (M/M_s) (where M is the magnetization and M_s is the saturation magnetization of a domain) near and around T_C [12]. In the high temperature limit, the conductivity is explained through the formation of small polarons around JT ions or the lattice bipolarons. The conductivity pattern, of course, can be described by the phenomenology $\rho = \rho_0 T^n \exp(U/k_B T)$ in all the cases of adiabatic or non-adiabatic polarons. Therefore, it appears that the general ρ–T pattern for all the samples can be fitted with a simple yet robust two-channel conduction model [22] which takes care of the ferromagnetism related metallic conduction below T_C and the activated hopping conduction above T_C whatever may be the actual conduction mechanism. The conductivity (σ) is given by

$$\sigma(T) = \alpha(M/M_s)^2 + (\beta/T^n)\exp(-U/k_B T) \tag{1}$$

where U is the activation barrier and α, β are constants. (M/M_s) is given by [23]

$$m(b,t) = B_J\left\{\frac{3J(m+b)}{(J+1)t}\right\} \tag{2a}$$

where B_J is the Brillouin function and is given by [23]

$$B_J(y) = \left\{\frac{2J+1}{2J}\right\}\coth\left\{\frac{(2J+1)y}{2J}\right\} - \left(\frac{1}{2J}\right)\coth\left(\frac{y}{2J}\right) \tag{2b}$$

where J is the total angular moment, b is the exchange field ($= B/\lambda M_s$; λ is the exchange coefficient and B is the magnetic field induction) and $t = T/T_C$. The solution to the equations (1) and (2) for resistivity $\rho(t) = 1/[m^2 + \exp(-t_0/t)]$ ($t_0 = U_0/k_B T_C = 2.5$ and $\alpha = \beta = 1$ are assumed) and magnetization $m(b,t)$ for different field values of b ($= 0.02$–0.25) is shown in figure 2. Fitting of the zero-field resistivity data for each of the samples is shown in figure 1 (solid lines). The list of the fitting parameters, α, β, T_C, $U/k_B T_C$ etc corresponding to each sample is given in table 1. Notable is the increase in fitting parameter

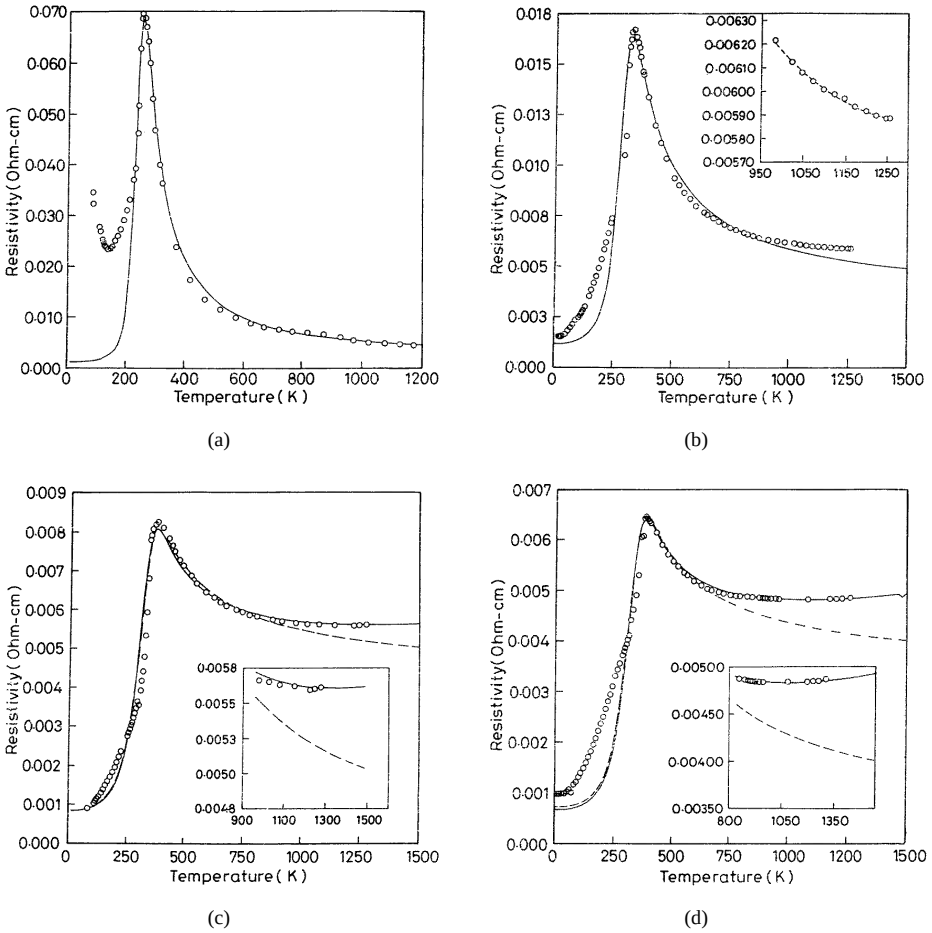

Figure 1. The resistivity (ρ) versus temperature (T) plots for the samples (a) $x = 0.16$, (b) $x = 0.20$, (c) $x = 0.25$, (d) $x = 0.30$, (e) $x = 0.40$, (f) $x = 0.45$, (g) $x = 0.50$. Hollow circles represent the actual data points while the solid lines represent the calculated patterns. Insets: the nature of resistivity versus temperature patterns at the higher temperature is shown.

T_C with the increase in x up to $x = 0.4$; T_C starts decreasing beyond that value of x. This is the reflection of enhanced Mn^{3+}–O^{2-}–Mn^{4+} ferromagnetism (through double exchange) because of the increase in Mn^{4+} concentration. Beyond $x = 0.4$, of course, Mn^{4+}–O^{2-}–Mn^{4+} antiferromagnetism (type G) starts dominating and as a result, T_C, once again, decreases. It is to be noted that the T_C reported here is obtained from the fitting of the theoretical ρ–T patterns with the experimental data points *and is not an experimental result in itself.* Such theoretical estimates of T_C turn out to be approximately 100 K lower than the actual peak temperatures T_p (which is observed experimentally) in the resistivity patterns. These peak temperatures are closer to the experimental Curie point found from magnetization studies. All these parameters are listed in table 1. The peak temperatures are comparable with the values observed by other researchers in the $La_{1-x}Sr_xMnO_3$ systems [24]. The discrepancy between the theoretical and experimental Curie points is probably the result of local (spatial)

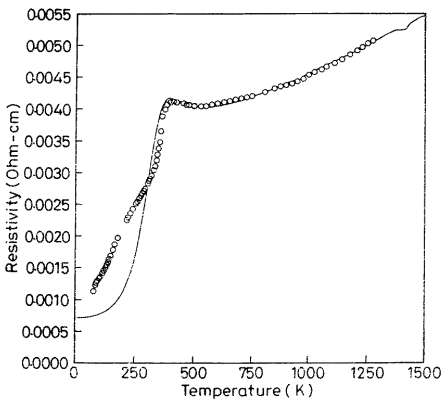

(e)

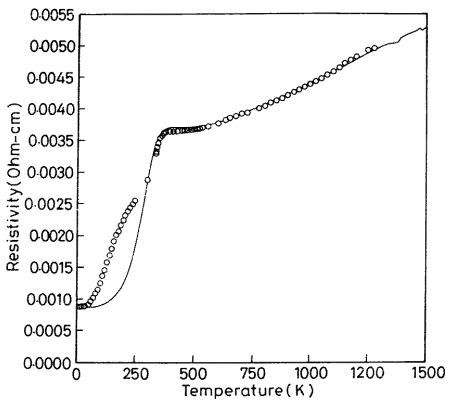

(f)

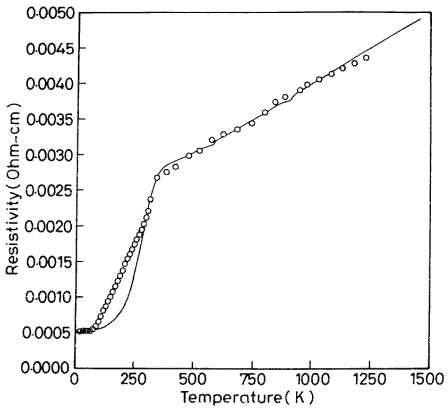

(g)

Figure 1. (Continued)

variations in the T_C among several clusters which lead to the broadening of the resistivity peak (or metal–insulator transition near T_C) and the ferromagnetic to paramagnetic transition. The local variation results from the inhomogeneity in the oxygen stoichiometry (or inhomogeneous distribution of oxygen) across the matrix. Hence, the fitting parameter T_C signifies the Curie point corresponding to the largest cluster in the matrix. For homogeneous samples, the fitting parameter T_C will be comparable to the experimental values. The resistivity peak, in such cases, will be much sharper than what has been observed in the present case. This point has been noted by others also, even in the context of thin films [22]. In spite of such discrepancy, the overall ρ–T patterns for all the samples could be fitted with the simple two-channel conduction equation and the fitting parameters rightly reveal the relative variation in the sample properties with the level of 'Sr' doping (x).

The activation barrier U decreases from 80.6 meV to 19 meV with the increase in x (0.16–0.50). The charge transport above T_C follows activated hopping from site to site. The origin of such activation barrier remains a bit controversial. As mentioned in the introduction section, at least, three mechanisms have so far been proposed in order to explain the conductivity and

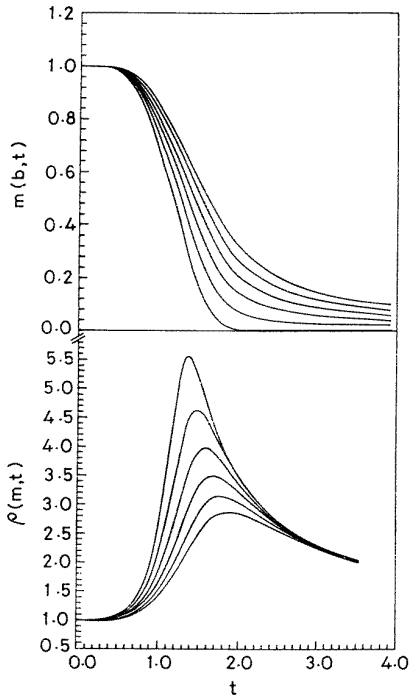

Figure 2. The variation in the normalized magnetization $m(b, t)$ and the resistivity $\rho(t)$ with the reduced temperature $t(= T/T_C)$ for different values of b (0.02, 0.066, 0.112, 0.158, 0.204, 0.25) is shown. For the $m(b, t)$ versus t plots (top plate), b increases from the inner curves towards the outer ones while for the $\rho(t)$ versus t plots (bottom plate) b increases from the outer curves towards the inner curves.

Table 1. List of important parameters used to describe the conductivity patterns.

x	α (ohm^{-1} cm^{-1})	β (ohm^{-1} cm^{-1})	U/k_BT_C	U (meV)	n	T_C (K)	T_p (K)	T^* (K)
0.16	865	476	5.5	80.6	—	170	256	—
0.20	850	290	2.37	46.0	—	225	337	—
0.25	1175	397.5	1.6	34.9	0.3	253	366	1223
0.30	1486	554.5	1.7	37.2	0.41	254	380	1080
0.40	1385	1005	1.68	37.9	0.8	262	390	548
0.45	1150	855	1.3	28.6	0.73	255	365	508
0.50	1800	850	0.9	19.0	0.72	245	360	410

magnetoresistivity near and above T_C: (i) formation of JT polarons [5], (ii) formation of spin polarons around JT-active ions [13] and (iii) formation of bipolarons [14]. While in the first case the splitting of the Mn^{3+} outer 3d levels and associated lattice distortion is proposed to be leading to the formation of the polarons, in the second case exchange coupling of the spin of the carriers with the ferromagnetic clusters (which are found to be dispersed within the paramagnetic matrix above T_C) is presumed to have localized the carriers. The third case proposes formation of the lattice bipolarons comprised of polarons around O^-. Strong coupling

of the bipolarons and their collapse through ferromagnetic exchange below T_C is proposed to be governing the conductivity and magnetoresistivity near and below T_C. Although, at this juncture, it is difficult to prove conclusively the nature of the conduction fluid below and above T_C, there seem to be quite a few concrete pieces of evidence of formation of JT polarons and the relevance of JT effect in this class of materials. Apart from the seminal works of Millis *et al* [5, 25], some other experimental evidence [6–9] also suggests the presence of JT distortions in this system. Louca *et al* [26] analysed the local distortion in $La_{1-x}Sr_xMnO_3$ ($0.0 < x < 0.5$) by pair-density functions (PDFs) using pulsed neutron diffraction data. This analysis has pointed out that the local distortion (which may have differences with the distortions observed over the entire crystallographic phase) is the JT type where four Mn–O bonds within a plane in $Mn^{3+}O_6$ octahedra are shortened ($\sim$1.95 Å) and the two others across the plane are stretched ($\sim$2.22 Å). The amount of distortion, of course, varies with the variation in doping level x. This distorted structure and the charge–lattice coupling as a result of that stabilizes the formation of JT polarons. The formation of JT polarons was highlighted by Zhao *et al* [6] as well. Such polarons seem to have given rise to the giant isotope effect as the electron bandwidth (W) varies as a result of the JT effect following $W \propto W_0 \exp(-E_{JT}/h\omega)$, where W_0 is the bare electron bandwidth and ω is the frequency of the optical phonons. The formation of JT polarons also gains support from the fact that the activation barrier estimated from the resistivity data is higher than that estimated from the recent thermopower data [9]. This is so because for conduction actual charge transport over the gap is necessary while particle–particle correlation can transfer the heat. Therefore, it appears that the activation barrier U in equation (2) actually represents the Jahn–Teller coupling energy E_{JT}. In figure 3, the variation of E_{JT} as a function of x is shown.

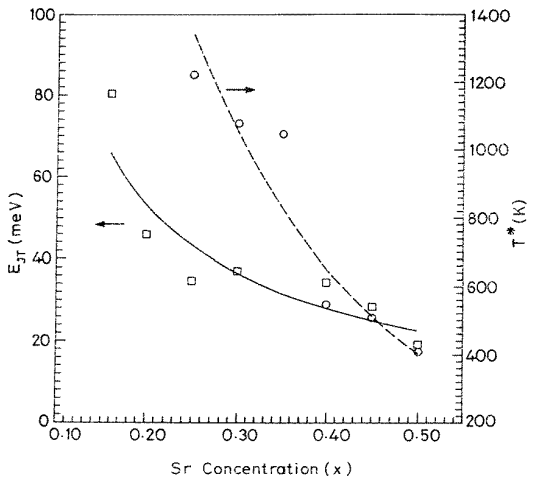

Figure 3. The variation in E_{JT} and T^* with the Sr concentration (x) is shown. Solid and dashed lines are guides to the eyes.

The drop in E_{JT} with the increase in x reflects the variation in the extent of JT coupling with the decrease in the number of JT-active Mn^{3+} ions. The estimated values are comparable with the values reported elsewhere [27]. Of course, these values are roughly one order of magnitude smaller than the true theoretical JT binding energy. Such discrepancy is probably the result of quantum fluctuation effect around the site of coupling.

Interestingly, the ρ–T pattern beyond T_C changes above a certain characteristic temperature T^* in these systems. Such change is not commensurate with any transition in magnetic behaviour. Therefore, it can be said that the nature of conduction in these materials above T_C does not have much correlation with the spin ordering. The re-entrant metallic ρ–T pattern above T^* can be fitted well using the temperature dependent prefactor in the second part of conduction equation (2). Since the temperature is varied over roughly two orders of magnitude, the regime changes from $k_BT < E_{JT}$ to $k_BT > E_{JT}$ which signals a cross-over in the resistivity behaviour. It reflects the saturation of charge carrier activation in the conduction band beyond T^*. Such a pattern has been observed in many Mott–Anderson localized systems [28]. The most plausible explanation for the re-entrant metallic ρ–T pattern could be the change in the extent of small polaron forming distortion. Small polarons, associated with the local distortion, gives way to large and extended polarons beyond T^*. There are, at least, two reasons to suggest such a mechanism: (i) the JT polaron binding energy and the temperature T^* appear to have a strong correlation with the number of JT-active Mn^{3+} ions. Both of them drop significantly with the drop in the JT-active ions. The drop in T^* with x is also shown in figure 3. It corroborates the results of the detailed structural studies [26]: the number of undistorted bonds in $Mn^{3+}O_6$ octahedra changes from four (in the case of parent $LaMnO_3$) to six (in the case of $SrMnO_3$ which does not contain any JT ion). (ii) The crystal structure, too, in this class of materials, undergoes a transition from a distorted one to the one of higher symmetry as a result of transition of the covalent bond ordering to some admixture (covalent + ionic) bonds at a transition temperature which is higher than T_C [29]. The small to large polaron transition and commensurate cross-over from incoherent to coherent polaron movement at a higher temperature is a natural phenomenon, operationally [30]. Because of the large scale atom movement, polarons with extended states and large bandwidth can be observed at a higher temperature. The coherent movement of the large polarons with only limited scattering gives rise to the re-entrant metallic conductivity beyond T^*. Normally, the bandwidth of such large polarons is higher than the disorder energy of the system and hence the polaron movement is not greatly affected by the disorder. This relaxation effect provides evidence of the formation of JT polarons and rules out the disordered spin scattering mechanism. It is to be noted, in this context, that the re-entrant metallic ρ–T pattern could as well be due to the unbinding and higher mobility of the bipolarons at higher temperatures. One cannot *a priori* rule out such a possibility. A structural transition study around T^* would provide conclusive evidence.

The nature of the conduction above T^* can be ascertained from the index n. It should be 1 or $\frac{3}{2}$ for adiabatic or non-adiabatic small polarons respectively. It appears, however, that for the low doping regime the ρ–T pattern is sublinear while with the increase in Sr concentration the pattern tends to become more linear. The discrepancy between the theoretical and experimental values of n could be due to spatial inhomogeneity within the sample. However, further study is necessary in this temperature regime to understand the characteristics of the conduction fluid.

4. Summary

In summary, the resistivity–temperature patterns of the $La_{1-x}Sr_xMnO_3$ ($0.1 < x \leqslant 0.5$) systems have been reported over a wide temperature regime 20–1273 K. The pattern follows a general trend of metallic below T_C and insulating above T_C. However, an interesting feature is the re-entrant metallic behaviour above a characteristic temperature T^* in the paramagnetic regime. This is possibly the result of relaxation of small polarons which form in these systems due to the Jahn–Teller effect. By using a simple two-channel conduction model we could fit the entire pattern of resistivity–temperature data and estimate the Jahn–Teller coupling energy E_{JT}. Both E_{JT} and T^* appear to vary significantly with the Mn^{3+} ion concentration. Beyond

T^*, the small polarons relax to large polarons (along with the structural transition to higher symmetry) which gives rise to the re-entrant metallic resistivity–temperature pattern. Such transition is not associated with any magnetic transition. Comprehensive structural transition study at such temperature range would provide evidence in support of this conjecture. Our data over such a wide temperature range may encourage detail consideration of the charge transport mechanisms in the high temperature limit.

Acknowledgments

The authors are pleased to acknowledge helpful discussion with Dr P Choudhury of CGCRI. One of the authors (DB) acknowledges the financial support from CSIR, Government of India, during this work. Partial support from MNES, Government of India, is also acknowledged.

References

[1] Von Helmolt R, Wecker J, Holzapfel B, Schulz L and Samwer K 1993 *Phys. Rev. Lett.* **71** 2331
[2] Jin S, Tiefel T H, McCormack M, Fastnacht R A, Ramesh R and Chen L H 1994 *Science* **264** 413
[3] Urushibara A, Moritomo Y, Arima T, Asamitsu A, Kido G and Tokura Y 1995 *Phys. Rev.* B **51** 14 103
[4] Zenner C 1951 *Phys. Rev.* **82** 403
Anderson P W and Hasegawa H 1955 *Phys. Rev.* **100** 675
de Gennes P G 1960 *Phys. Rev.* **118** 141
[5] Millis A J, Littlewood P B and Shraiman B I 1995 *Phys. Rev. Lett.* **75** 5144
[6] Zhao G-m, Conder K, Keller H and Mueller K A 1996 *Nature* **381** 676
[7] Shengelaya A, Zhao G-m, Keller H and Mueller K A 1996 *Phys. Rev. Lett.* **77** 5296
[8] Kaplan S G, Quijada M, Drew H D, Tanner D B, Xiong G C, Ramesh R, Kwon C and Venkatesan T 1996 *Phys. Rev. Lett.* **77** 2081
[9] Palstra T T M, Ramirez A P, Cheong S-W, Zegarski B R, Schiffer P and Zaanen J 1997 *Phys. Rev.* B **56** 5104
[10] Ju H L, Sohn H-C and Krishnan K M 1997 *Phys. Rev. Lett.* **79** 3230
[11] Okimoto Y, Katsufuji T, Ishikawa T, Arima T and Tokura Y 1997 *Phys. Rev.* B **55** 4206
[12] Imada M, Fujimori A and Tokura Y 1998 *Rev. Mod. Phys.* **70** 1039
[13] See, for example, Goodenough J B 1998 *Annu. Rev. Mater. Sci.* **28** 1
[14] Alexandrov A S and Bratkovsky A M 1999 *Phys. Rev. Lett.* **82** 141
[15] Chakraborty A, Devi P S, Roy S and Maiti H S 1994 *J. Mater. Res.* **9** 986
Chakraborty A, Devi P S and Maiti H S 1994 *Mater. Lett.* **20** 63
[16] Maiti H S, Chakraborty A and Paria M K 1993 *Proc. 3rd Int. Symp. on Solid Oxide Fuel Cells* ed S C Singhal and H Iwahara (Pennington, NJ: The Electrochemical Society) p 190
[17] Chakraborty A, Devi P S and Maiti H S 1995 *J. Mater. Res.* **10** 918
Chakraborty A, Bhattacharya D and Maiti H S 1997 *Phys. Rev.* B **56** 8828
[18] Anderson I G K, Anderson E K, Norby P and Skou E 1994 *J. Solid State Chem.* **113** 320
[19] See, for example, Minh N Q 1993 *J. Am. Ceram. Soc.* **76** 563
[20] Kuo J H, Anderson H U and Sparlin D M 1990 *J. Solid State Chem.* **87** 55
[21] Yamada Y, Hino O, Nohdo S, Kanao R, Inami T and Katano S 1996 *Phys. Rev. Lett.* **77** 904
[22] Nunez Regueiro J E and Kadin A M 1996 *Appl. Phys. Lett.* **68** 2747
[23] Cullity B D 1972 *Introduction to Magnetic Materials* (Reading, MA: Addison-Wesley)
[24] Mahendiran R, Tiwany S K, Raychaudhuri A K, Ramakrishnan T V, Mahesh R, Rangavittal N and Rao C N R 1996 *Phys. Rev.* B **53** 3348
[25] Millis A J, Shraiman B I and Mueller R 1996 *Phys. Rev. Lett.* **77** 175
[26] Louca D, Egami T, Brosha E L, Roeder H and Bishop A R 1997 *Phys. Rev.* B **56** R8475
[27] See, for example, Ramakrishnan T V 1998 *Phil. Trans. R Soc.* A **356** 41
[28] Mott N F and Davis E A 1979 *Electronic Processes in Non-Crystalline Systems* (London: Clarendon)
[29] Goodenough J B 1955 *Phys. Rev.* **100** 564
[30] Emin D 1995 *Polarons and Bipolarons in High-T_C Superconductors and Related Materials* ed E K H Salje, A S Alexandrov and W Y Liang (Cambridge: Cambridge University Press)